ISBN: 978-3-95450-132-8 doi:10.18429/JACoW-IPAC2014-MOPRO083

DESIGN STUDY OF HIGH BRILLIANT OPTICS AT THE SPRING-8 STORAGE RING

Y. Shimosaki#, T. Aoki, K. Fukami, K. Kaneki, K. Kobayashi, M. Masaki, C. Mitsuda, H. Ohkuma, M. Shoji, K. Soutome, S. Takano, M. Takao, JASRI / SPing-8, Hyogo, Japan

Abstract

At the SPring-8 storage ring, design study of beam optics concentrating particularly on increasing brilliance, not flux density, is in progress besides continuous efforts of increasing both brilliance and flux density for the user optics. The natural emittances are theoretically reduced from 2.41 nmrad at 8 GeV to 2.27 nmrad (8 GeV), 1.78 nmrad (7 GeV) and 1.33 nmrad (6 GeV) by utilizing an emittance damping effect by the insertion devices. The designed optics has experimentally been examined at 6 GeV, and the electron beam parameters have been confirmed by measurements at the diagnostics beamlines.

INTRODUCTION

The SPring-8 is a third generation synchrotron light source to provide brilliant hard X-rays of the order of 10^{20} photons / sec / mm^2 / mrad^2 / 0.1 % B.W. with electrons of 100 mA at 8 GeV. On May 2013, the user optics (UO) lowering the natural emittance from 3.49 nmrad to 2.41 nmrad was opened to user operation [1]. The lattice function of the new UO with 2.41 nmrad was optimized for increasing not only the brilliance but also the flux density. Moreover, in order to provide the stable photon beam intensity during the user-time, the lattice function at each straight section are optimized for the emittance not to be changed drastically by the radiation excitation and damping due to insertion devices (IDs) [1, 2].

Besides these studies for the UO, a feasibility study for an optics specialized particularly for increasing the brilliance, not the flux density, which is called a high brilliant optics (HBO) in this paper, has been examined in order not only to study a strategy of a design for HBO but also to confirm the potential performance of the SPring-8. A HBO has been optimized for (1) decreasing the electron emittance, (2) enhancing the emittance damping by IDs in contrast to the present UO, and (3) decreasing the effective photon emittance at the light source point of IDs which is inversely proportional to the brilliance. An emittance damping ratio and a growth ratio of a momentum deviation (1σ) resulted from IDs, of which the former is tunable by selecting the lattice function, are given by

$$\frac{\varepsilon\left(\beta_x, D_x\right)}{\varepsilon_0} = \frac{1+\sum_{ID}\frac{2C_q\gamma^2}{3\pi^2\varepsilon_0}\frac{L_u\rho_0}{\rho_u^3}\left[\frac{K_u^2}{5\gamma^2}\left(\beta_x+\frac{L_u^2}{12\beta}\right)+\frac{D_x^2}{\beta_x}\right]}{1+\sum_{ID}\frac{L_u}{4\pi\rho_0}\left(\frac{\rho_0}{\rho_u}\right)^2},$$

$$\frac{\delta}{\delta_0} = \sqrt{\left\{1+\sum_{ID}\frac{2L_u}{3\pi^2\rho_0}\left(\frac{\rho_0}{\rho_u}\right)^3\right\}\left\{1+\sum_{ID}\frac{L_u}{4\pi\rho_0}\left(\frac{\rho_0}{\rho_u}\right)^2\right\}^{-1}},$$

where C_q = 3.84 x 10^{-13} m, γ is the Lorentz factor, (ε_0, δ_0) and (ε, δ) are the natural emittance and the momentum deviation (1σ) for opened and closed gaps of IDs, respectively [3]. ρ_0 is the bending radius. β and D are the beta function and the dispersion function at the light source point, respectively. L_u, $K_u = \lambda_u\gamma / 2\pi\rho_u$ and λ_u are the length, the strength parameter and the period of the ID, respectively. An effective photon emittance at a light source point of an ID is defined by a convolution of photon emittance with the electron emittance as

$$\varepsilon_p\left(\beta_x,\beta_y,D_x\right) = \Sigma_x\left(\beta_x,D_x\right)\Sigma_x'\left(\beta_x,D_x\right) \times \Sigma_y\left(\beta_x,\beta_y,D_x\right)\Sigma_y'\left(\beta_x,\beta_y,D_x\right),$$

$$\Sigma_x\left(\beta_x,D_x\right) = \sqrt{\varepsilon\left(\beta_x,D_x\right)\beta_x\left(1+\kappa\right)^{-1}+D_x^2\delta^2+\sigma_p^2},$$

$$\Sigma_x'\left(\beta_x,D_x\right) = \sqrt{\varepsilon\left(\beta_x,D\right)\left(1+\kappa\right)^{-1}\beta_x^{-1}+\sigma_p'^2},$$

$$\Sigma_y\left(\beta_x,\beta_y,D_x\right) = \sqrt{\kappa\varepsilon\left(\beta_x,D\right)\beta_y\left(1+\kappa\right)^{-1}+\sigma_p^2},$$

$$\Sigma_y'\left(\beta_x,\beta_y,D_x\right) = \sqrt{\kappa\varepsilon\left(\beta_x,D\right)\left(1+\kappa\right)^{-1}\beta_y^{-1}+\sigma_p'^2},$$

where κ is the emittance coupling ratio, σ_p and σ_p' are the size and divergence of the single photon, respectively.

OPTICS DESIGN

The main parameters of the designed HBO at 6, 7 and 8 GeV are listed in Table 1, and the lattice functions are shown in Fig. 1, wherein κ is set to 0.2 % and 21 SPring-8 standard undulators (L_u = 4.5 m, K_u = 2.5, and λ_u = 32 mm) are assumed to be utilized for the emittance damping. It is noted that the magnet positions and polarities are unchanged and the strength of magnetic fields are optimized within the specifications.

The lattice functions of the present UO have been optimized by setting β_x and D at the light source point to the larger values than those of the past 3.49 nmrad optics to increase not only the brilliance but also the flux density, and for the emittance not to be changed drastically by IDs. For the HBO to enhance the emittance damping by IDs, and to decrease the effective photon emittance, β_x, β_y and D are set to the lower values than those of the present UO; The effective photon emittance of 10 keV photon for the HBO designed at 6 GeV (HBO-6) becomes 1 / 2.5 times smaller than the present UO at 8 GeV.

#shimosaki@spring8.or.jp

ISBN: 978-3-95450-132-8 doi:10.18429/JACoW-IPAC2014-MOPRO083

The brilliance and flux density predicted by SPECTRA [4] are shown in Fig. 2, where the stored current of 200 mA is assumed for the HBO-6 though we can store the electrons of 200 mA but cannot provide the photons emitted from 200 mA for users from viewpoint of the radiation safety at the present SPring-8, because its emittance of 1.33 nmrad is larger by a degree of magnitude than that of an ultra-low emittance ring [5] and the sufficiently long beam lifetime is expected and the intrabeam scattering is negligible for the beam current. Moreover, while the 21 standard IDs are assumed for the emittance damping as be mentioned above, a short-period undulator of λ_u = 23 mm, L_u = 4.5 m and K_u = 2.3, where the minimum gap of 5.5 mm is assumed from the vertical beta function at the ID and then λ_u of 23 mm is determined by the Halbach's equation [6] for satisfying K_u = 2.3 at the gap of 5.5 mm, is assumed to calculate the brilliance and flux density at the HBO-6 in order to provide the hard X-ray at 6 GeV. Figures 2 (a) and (b) show that the HBO-6 should provide 4.8 times higher brilliance and 2.5 times higher flux density for 10 keV photons than those of the present UO with the help of the emittance damping.

Table 1: Main Parameters of HBO

	HBO			UO
E (GeV)	6	7	8	8
ε (nmrad) / ε_0 (nmrad)	1.33 / 1.78	1.78 / 2.08	2.27 / 2.52	2.27 / 2.41
δ (%) / δ_0 (%)	0.087/ 0.082	0.098/ 0.096	0.110 / 0.109	0.110 / 0.109
(β_x (m), β_y (m))	(30.0, 3.8)	(31.2, 2.9)	(28.0, 2.3)	(31.2, 5.0)
D (m)	0.09	0.12	0.13	0.15
ε_p for 10 keV photon (10^{-21} m^{2}rad^2)	25.6	35.4	46.5	64.7

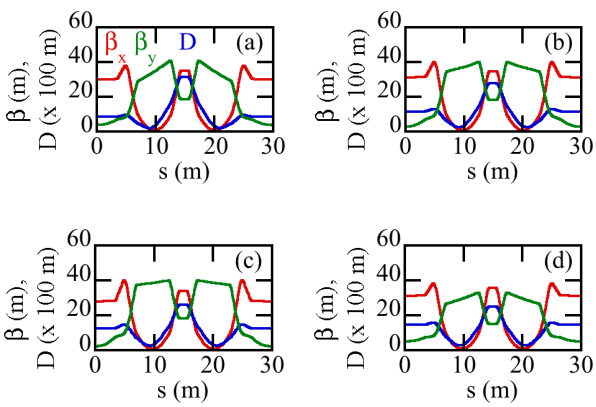

Figure 1: Lattice functions of HBO at (a) 6 GeV, (b) 7 GeV and (c) 8 GeV, and (d) UO.

In order to apply the designed HBO-6 to the present SPring-8 storage ring, the nonlinear optics has been optimized. The dynamic aperture calculated by CETRA [7] is shown in Fig. 3, where the errors estimated by the response matrix analysis are taken into account. We see that the horizontal dynamic aperture is larger than ±10 mm, which is the required value for beam injection.

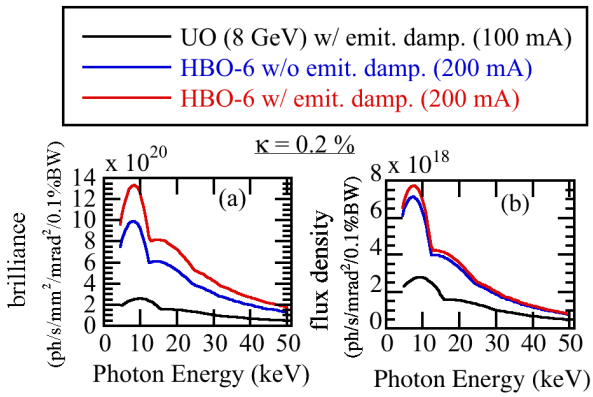

Figure 2: (a) Brilliance and (b) flux density at HBO-6 and UO (SPECTRA). κ = 0.2 %.

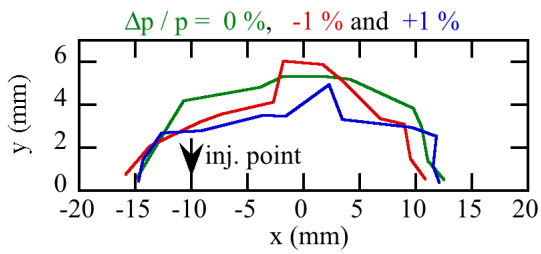

Figure 3: Dynamic aperture at HBO-6 (CETRA) .

ACHIEVED PERFORMANCE

The beam tests have been carried out for the HBO-6. The stored current was 60 mA and the amplitude of RF voltage was set to 9.8 MV in order to suppress the beam instability caused in the longitudinal direction. The longitudinal beam instability will be suppressed by the newly developed kicker system [8], and then we will hopefully increase the stored current.

In order to qualitatively confirm the emittance damping effect by the IDs, the electron beam size and the photon beam size were observed at the accelerator diagnostics beamlines I and II (BL38B2 and BL05SS) by changing the gaps of the IDs (see Table 2). The electron beam size was simultaneously measured by a newly installed X-ray pinhole camera with the dipole source 29B2. The measured sizes are listed in Table 3. The emittance and the momentum deviation (1σ) are determined by the least squares method with the lattice functions estimated from the response matrix analysis and the measured sizes of both the electron and the photon beams. The evaluated emittance and momentum deviation (1σ) are shown in

ISBN: 978-3-95450-132-8 doi:10.18429/JACoW-IPAC2014-MOPRO083

Fig.4. The resulting value of the horizontal emittance shows a good agreement with the design. The momentum deviation (1σ) is found to be larger than the theoretical one. We will cross-check the momentum deviation (1σ) by measuring the bunch length.

Table 2: Gap Conditions for Measurements of Electron Beam Size and Photon Beam Size

	Gap condition
RUN-1	Gap is fully opened at all IDs.
RUN-2	Min. gap at ID19, 36, 37, 39, 41, 44, 46, and 47.
RUN-3	In addition to RUN-2, min. gap at ID20, 22, 28, 29, 32, 33, and 35.
RUN-4	In addition to RUN-3, min. gap at ID03, 09, 11, 12, 13, and 16.

Table 3: Photon Beam Size Measured at BL05SS (ID05), and Electron Beam Size Measured at BL38B2 (Bending) and that with X-ray Pinhole Camera at 29B2 (Bending)

	RUN-1	**RUN-2**	**RUN-3**	**RUN-4**
ID05 (mm)	0.880	0.814	0.798	0.799
29B2 (μm)	88.386	87.263	86.518	85.515
38B2 (μm)	87.725	84.228	83.677	84.231

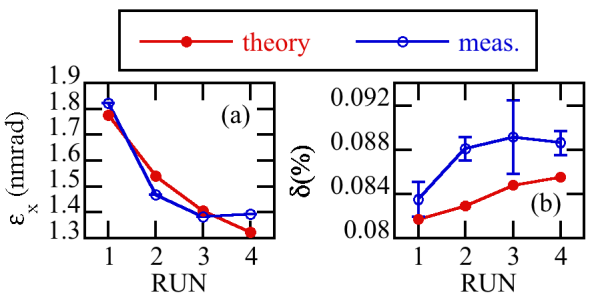

Figure 4: Evaluated (a) emittance and (b) momentum deviation (1σ) dependent on gap condition in Table 2.

The results of the X-ray beam imager [9] measured at BL38B2 are shown in Fig. 5. The vertical emittance of 7.3 pmrad at RUN-1 and 5.1 pmrad at RUN-4 are determined by the measured beam size and the lattice functions estimated from the response matrix analysis.

The horizontal projection of the beam profile of the 7.167 keV photon measured at 92.2 m from the light source point of ID05 is shown in Fig. 6, which is normalized by the stored current. The peak intensity at RUN-4 becomes 1.1 times higher than that at RUN-1, which is consistent with the ratio of the flux density between RUN-1 and 4 calculated by SPECTRA.

Concerning the machine conditions, the normal injection efficiency of 74 % was achieved. The beam lifetime was 63.3 hours at RUN-4, when the stored current was 54.4 mA and the bunch filling was 160 bunch trains x 12, which corresponds to about 17 hours at 200 mA. After optimizing the machine conditions, the photon beam performance such as the flux density and the nano-focusing will be verified.

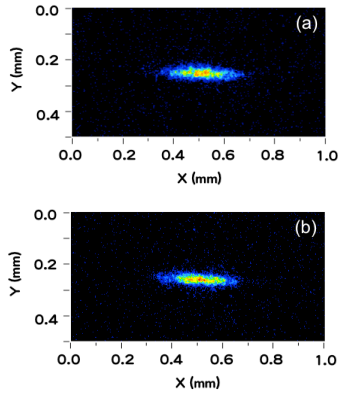

Figure 5: X-ray beam image measured at BL38B2. (a) RUN-1 and (b) RUN-4.

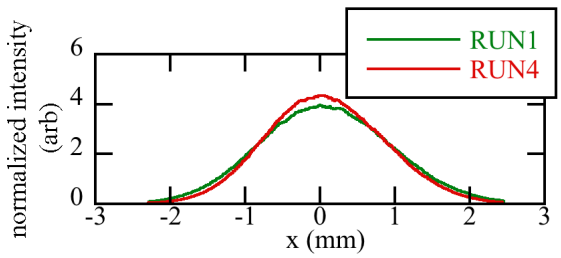

Figure 6: Horizontal projection of photon beam profile measured at 92.2 m from light source point of ID05.

REFERENCES

[1] Y. Shimosaki et al., IPAC13, MOPEA027.
[2] Y. Shimosaki et al., IPAC12, TUPPC013.
[3] e.g., NLS II Conceptual Design Report, pp. 6-2.
[4] T. Tanaka and H. Kitamura, SPECRA code ver. 9.02 (2012).
[5] e.g., SPring-8 II Conceptual Design Report, to be published.
[6] A. W. Chao and M. Tigner, "Handbook of Accelerator Physics and Engineering", World Scientific.
[7] J. Schimizu, et al., Proc. of 13th Symp. on Accel. Sci. and Tech. Osaka, Japan (2001), pp.80-82.
[8] M. Masaki, private communication.
[9] S. Takano et al., Nucl. Instrum. Meth. A 556, 357 (2006).